Temperature-modulation analysis of superconductivity-induced transfer of in-plane spectral weight in $Bi_2Sr_2CaCu_2O_8$

A. B. Kuzmenko, H. J. A. Molegraaf, F. Carbone, and D. van der Marel
Département de Physique de la Matière Condensée, Universitée de Genève, CH-1211 Genève 4, Switzerland
(Received 7 April 2005; revised manuscript received 27 June 2005; published 5 October 2005)

We examine the superconductivity-induced redistribution of optical spectral weight in $Bi_2Sr_2CaCu_2O_8$ near optimal doping using a detailed Kramers-Kronig consistency analysis of the kink (slope change) at T_c of the temperature-dependent optical spectra, published earlier [H. J. A. Molegraaf *et al.*, Science **295**, 2239 (2002)]. We demonstrate that the temperature dependence of the complex dielectric function at high frequencies (above 0.75 eV) imposes the most stringent limits on the possible changes of the low-frequency integrated spectral weight. The presented calculations provide additional arguments, supporting the previous conclusion about a superconductivity-induced increase of the integrated low-frequency spectral weight below T_c. The Ferrell-Glover-Tinkham sum rule is not satisfied well above 2.5 eV, which indicates that this increase is caused by the transfer of spectral weight from the interband to the intraband region and only partially by the narrowing of the Drude peak.

DOI: 10.1103/PhysRevB.72.144503 PACS number(s): 74.25.Gz, 74.20.Mn, 74.72.Hs, 78.20.Ci

I. INTRODUCTION

The problem of superconductivity- (SC-) induced spectral weight (SW) transfer in the high-T_c cuprates is in the focus of numerous experimental[1–13] and theoretical[14–31] studies. Of special interest is the charge carrier optical spectral weight[21]

$$W_{intra} \equiv \int_0^{\infty} \sigma_{1,intra}(\omega)d\omega = \frac{\pi e^2}{\hbar^2 VN}\sum_k n_k \frac{\partial^2 \epsilon_k}{\partial k_x^2}, \qquad (1)$$

where $\sigma_{1,intra}(\omega)$ denotes the optical conductivity due to the intraband transitions, including the condensate δ peak in the SC state, V the unit cell volume, ϵ_k the band dispersion, n_k the momentum occupation number, and N the number of momentum states. The influence of the superconducting transition on the intraband spectral weight is one of the key experimentally verifiable predictions which distinguish different scenarios of high-T_c superconductivity. This is most evident in the nearest-neighbor tight-binding model,[21,32] where the changes of W_{intra} and of the electronic kinetic energy $E_{kin}=(2/N)\Sigma_k n_k \epsilon_k$ are thus simply related (a is the in-plane lattice constant):

$$\Delta W_{intra} = -\frac{\pi e^2 a^2}{2\hbar^2 V}\Delta E_{kin}. \qquad (2)$$

While the Bardeen-Cooper-Schrieffer (BCS) scenario implies an increase of the kinetic energy in the SC state and a corresponding decrease of W_{intra}, the theories of unconventional superconductivity in the cuprates predict exactly the opposite.[14,15] Beyond the nearest-neighbor approximation one should directly compare Eq. (1) with experiment.[12]

In practice, one measures the low-frequency integrated SW

$$W(\Omega_c, T) = \rho_s(T) + \int_{0^+}^{\Omega_c} \sigma_1(\omega, T)d\omega, \qquad (3)$$

where $\rho_s(T)$ is the spectral weight of the condensate, $\sigma_1(\omega, T)$ is the real part of the optical conductivity, and the cutoff energy Ω_c represents the scale of scattering of the intraband (Drude) excitations. Although strongly related to the total intraband SW, this is not exactly the same as Eq. (1), since the intraband and interband optical regions actually overlap. Care thus should be taken[3] not to confuse the changes of $W(\Omega_c, T)$ due to the real change of $W_{intra}(T)$ and the ones due to the narrowing of the intraband peak.

Molegraaf *et al.*[1] reported the SC-induced increase of the intraband spectral weight in optimally doped (T_c=88 K) and underdoped (T_c=66 K) single crystals of $Bi_2Sr_2CaCu_2O_8$ (Bi2212) based on combined ellipsometry and reflectivity measurements. Santander-Syro *et al.*[2] independently arrived at the same conclusions by analyzing reflectivity spectra of high-quality Bi2212 films. A recent report of the opposite result for optimally doped $YBa_2Cu_3O_{6.9}$ (Y123, T_c=92.7 K) and slightly underdoped Bi2212 (T_c=86 K) (Ref. 3) has prompted us to present in the current paper, in detail, an alternative analysis of the data reported in Ref. 1. It confirms the original conclusions and can also be useful for the analysis of future data of a similar nature.

In order to numerically decouple the superconductivity-induced changes of the optical properties from the temperature dependences, already present in the normal state (such as a gradual narrowing of the Drude peak), we apply the slope-difference analysis, developed in Ref. 11, which is closely related to the well-known temperature-modulation technique.[33,34] It appears that any realistic model, which satisfactorily fits the total set of experimental data (reflectivity below 0.75 eV and ellipsometrically obtained real and imaginary parts of the dielectric function at higher energies), gives an *increase* of $W(\Omega_c, T)$ below T_c. Moreover, all attempts to

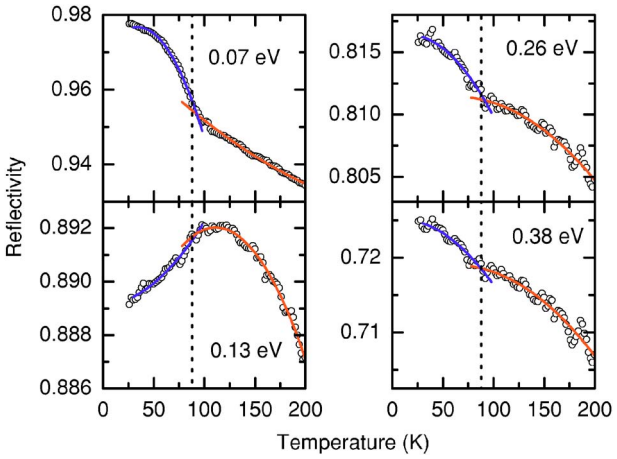

FIG. 1. (Color online) Temperature-dependent reflectivity of Bi2212 close to optimal doping (T_c=88 K) for selected frequencies in the infrared range. The dots are the data points, and the blue (red) solid curves are polynomial fits to the temperature dependence below (above) T_c, used to produce the kink (slope difference) values. The transition temperature is marked by the vertical dotted line.

do the same fitting with an artificial constraint that the SC-induced change of $W(\Omega_c,T)$ be negative, or even zero, failed to fit the data, despite using flexible multioscillator models.[35] Importantly, the ellipsometrically measured real and imaginary parts of the dielectric function, $\epsilon_1(\omega)$ and $\epsilon_2(\omega)$, *at high frequencies* provide the most stringent limits on the possible change of the *low-frequency* spectral weight $W(\Omega_c,T)$, due to the Kramers-Kronig (KK) relations.

Finally, we discuss whether the SC-induced increase of $W(\Omega_c,T)$ is caused by the extra narrowing of the Drude peak below T_c or by removal of the SW from the interband region. We find an extra narrowing of the Drude peak, in agreement with Ref. 3. However, this narrowing is too small to explain the increase of the low-frequency spectral weight, which suggests that there is a sizable spectral weight transfer from the range of the interband transitions.

II. SUPERCONDUCTIVITY-RELATED SPECTRAL CHANGES

As described in Ref. 1, the normal-incidence reflectivity $R(\omega)$ was measured between 200 and 6000 cm^{-1} (from 25 meV to 0.75 eV) and real and imaginary parts of dielectric function, $\epsilon_1(\omega)$ and $\epsilon_2(\omega)$, were obtained by spectroscopic ellipsometry from 6000 to 36 000 cm^{-1} (0.75–4.5 eV).

In Figs. 1 and 2 we display the temperature dependence of reflectivity and $\epsilon_{1,2}(\omega,T)$, respectively, for selected photon energies. The complex dielectric constant changes as a function of temperature in the entire range from 0 to 300 K. For high frequencies (larger than ~0.25 eV) the variation as a function of temperature is essentially proportional to T^2. The same temperature dependence has been observed in other cuprate superconductors—for example,[36]

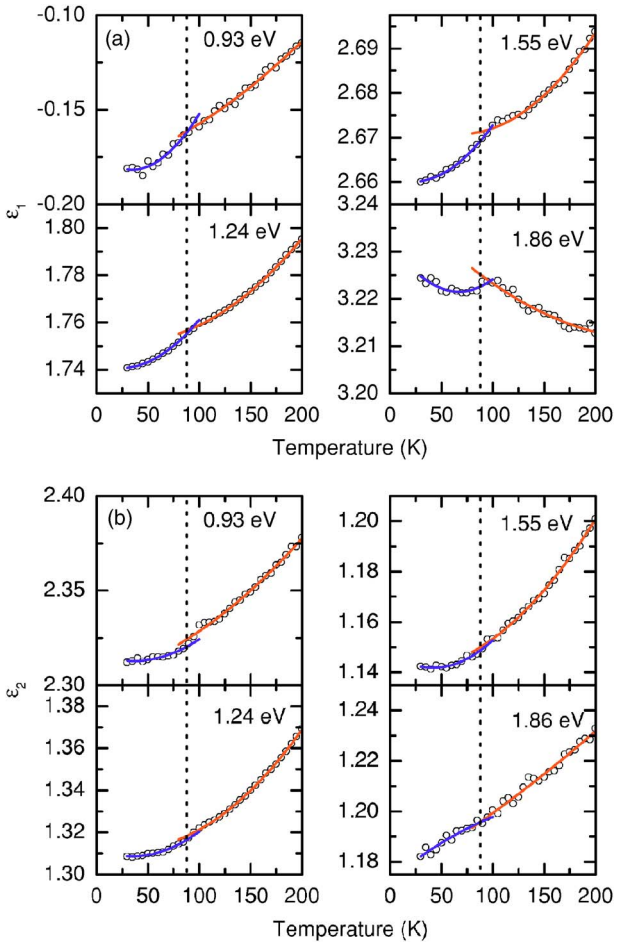

FIG. 2. (Color online) Temperature-dependent ellipsometrically measured $\epsilon_1(T)$ (a) and $\epsilon_2(T)$ (b) of Bi2212 close to optimal doping (T_c=88 K) for selected frequencies. The dots are the data points, and the blue (red) solid curves are polynomial fits to the temperature dependence below (above) T_c, used to produce the kink (slope difference) values. Not all temperature data points are shown. The transition temperature is marked by the vertical dotted line.

$La_{2-x}Sr_xCuO_4$—and has been explained quantitatively using the Hubbard model.[37] For low frequencies (below ~0.1 eV) the optical conductivity has a very large intraband contribution, with a dissipation increasing linearly with temperature, which causes a nonmonotonous temperature dependence of ϵ_1 and ϵ_2. In particular, it was found[38] that $1/[T\sigma_1(\omega)]$ is equal to a constant plus a term proportional to T^{-2}. The gradual decrease of the high-frequency conductivity with cooling down is also expected due to the reduction of the electron-phonon scattering.[39]

The onset of superconductivity is marked by clear kinks (slope changes) at T_c of the measured optical quantities (Figs. 1 and 2). An exciting feature of the high-T_c cuprates is that the kinks are seen not only in the region of the SC gap, but also at much higher photon energies (at least up to 2.5 eV in Ref. 1). It means that the formation of SC long-range order causes a redistribution of the spectral weight across a very large spectral range, a fact which several groups agree upon.[1–3,34,40]

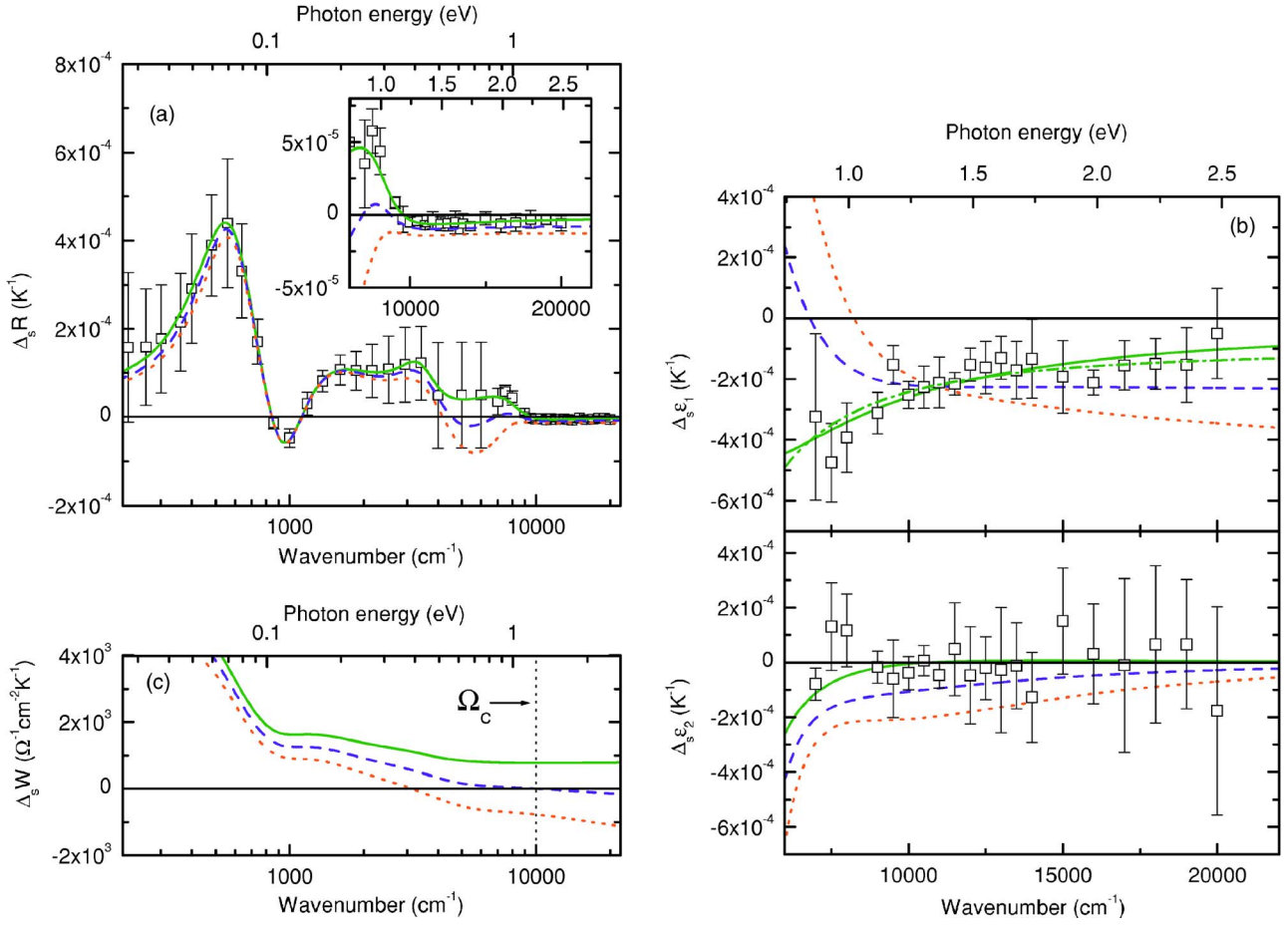

FIG. 3. (Color online) The spectral dependence of the slope difference $\Delta_s R(\omega)$ (a) and $\Delta_s \epsilon_1(\omega)$ and $\Delta_s \epsilon_2(\omega)$ (b). Data points show the kink value, derived from the temperature-dependent curves (Figs. 1 and 2) as described in Appendix A. Only a few data points of $\Delta_s R(\omega)$ out of all used in the analysis are shown. The line show different fits, as described in the text. The solid green curve indicates the best fit of $\Delta_s R(\omega)$, $\Delta_s \epsilon_1(\omega)$, and $\Delta_s \epsilon_2(\omega)$ simultaneously, giving $\Delta_s W(\Omega_c) \approx +770\ \Omega^{-1}\ \mathrm{cm}^{-2}\ \mathrm{K}^{-1}$ [the SC-induced *increase* of $W(\Omega_c)$]. The dashed blue and dotted red curves are the best fits of the same data with an artificial constraint $\Delta_s W(\Omega_c)=0$ and $-770\ \Omega^{-1}\ \mathrm{cm}^{-2}\ \mathrm{K}^{-1}$, respectively. One can see that both constraints are incompatible with the data. The green dash-dotted line is the best fit of $\Delta_s \epsilon_1(\omega)$ by the formula $-A\omega^{-2}+B$. The integrated spectral weight $\Delta_s W(\omega)$ (c) for all three fits is shown by the same colors. The inset of panel (a) shows $\Delta_s R(\omega)$ calculated from the ellipsometrically measured dielectric function from 0.75 to 2.75 eV on an expanded vertical scale.

An essential aspect of the data analysis is the way to separate the superconductivity-induced changes of the optical constants from the temperature-dependent trends, observed above T_c. A similar problem is faced in the specific-heat experiments,[41,42] where the superconductivity-related structures are superimposed on a strong temperature-dependent background. Let us introduce a slope-difference operator Δ_s, which measures the slope change (kink) at T_c (Ref. 11):

$$\Delta_s f(\omega) \equiv \left.\frac{\partial f(\omega,T)}{\partial T}\right|_{T_c+\delta} - \left.\frac{\partial f(\omega,T)}{\partial T}\right|_{T_c-\delta}, \qquad (4)$$

where f stands for any optical quantity. It properly quantifies the effect of the SC transition, since the normal-state trends are canceled out.[43] Since Δ_s is a linear operator, the KK relation is valid for the slope-difference spectra:

$$\Delta_s \epsilon_1(\omega) = 8\mathrm{P}\int_0^\infty \frac{\Delta_s \sigma_1(x)}{x^2-\omega^2}dx. \qquad (5)$$

In order to detect and measure a kink as a function of temperature as well as to establish whether or not the kink is seen at T_c the spectra must be measured using a fine temperature resolution. A resolution of 2 K or better was used in the entire range from 10 to 300 K which enables us to perform a reliable slope-difference analysis.

The data points in Figs. 3(a) and 3(b) show $\Delta_s R(\omega)$, $\Delta_s \epsilon_1(\omega)$, and $\Delta_s \epsilon_2(\omega)$, obtained from the directly measured temperature-dependent curves shown in Fig. 1 and 2. The details of the corresponding numerical procedure and the determination of the error bars are described in Appendix A.

One can see that $\Delta_s \epsilon_1(\omega)$ is *negative* and its absolute value is strongly decreasing as a function of frequency. In the same region, $\Delta_s \epsilon_2(\omega)$ is almost zero (within our error bars). Intuitively, it already suggests that the low-frequency inte-

grated spectral weight $W(\Omega_c,T)$ is likely to increase in the SC state. Indeed, in the simplest scenario, when the extra SW is added at zero frequency, one has $\Delta_s\epsilon_1(\omega)=-8\Delta_s W(0+)\omega^{-2}$. This formula becomes approximate if changes also take place at finite frequencies. However, the approximation is good if the most significant changes $\Delta_s\sigma_1$ occur only below $\omega_1 \ll \omega$ and above $\omega_2 \gg \omega$. This follows from the exact expansion[44] of Eq. (5), valid for $\omega_1 < \omega < \omega_2$:

$$\Delta_s\epsilon_1(\omega) = -\sum_{j=0}^{\infty}\frac{A_j}{\omega^{2+2j}} + \Delta_s\tilde{\epsilon}_1(\omega) + \sum_{j=0}^{\infty} B_j\omega^{2j}, \qquad (6)$$

where

$$A_j \equiv 8\int_0^{\omega_1} x^{2j}\Delta_s\sigma_1(x)dx,$$

$$B_j \equiv 8\int_{\omega_2}^{\infty}\frac{\Delta_s\sigma_1(x)}{x^{2+2j}}dx,$$

$$\Delta_s\tilde{\epsilon}_1(\omega) \equiv 8\mathrm{P}\int_{\omega_1}^{\omega_2}\frac{\Delta_s\sigma_1(x)}{x^2-\omega^2}dx.$$

For $\omega_1=0.8$ eV and $\omega_2=2.5$ eV we can calculate $\Delta_s\tilde{\epsilon}_1(\omega)$ directly from the measured $\Delta_s\sigma_1(\omega)$. It turns out that $|\Delta_s\tilde{\epsilon}_1(\omega)|<10^{-4}$ K^{-1}, while the average value is indistinguishable from zero. In this situation we can neglect $\Delta_s\tilde{\epsilon}_1(\omega)$, compared to the contributions from the low and high frequencies. Thus, to leading order,

$$\Delta_s\epsilon_1(\omega) \approx -A_0\omega^{-2} + B_0 = -8\Delta_s W(\omega_1)\omega^{-2} + \Delta_s\epsilon_\infty, \quad (7)$$

where $\epsilon_\infty = 8\int_{\omega_2}^{\infty}\sigma_1(\omega)\omega^{-2}d\omega$ is the integrated oscillator strength of all optical excitations above ω_2.

The best fit of $\Delta_s\epsilon_1(\omega)$ in the spectral region (0.8–2.5 eV) with Eq. (7) is shown by the green dash-dotted line in Fig. 3(b). It gives[45] $\Delta_s W(\Omega_c)\approx+360\ \Omega^{-1}\,\mathrm{cm}^{-2}\,\mathrm{K}^{-1}$ and $\Delta_s\epsilon_\infty \approx -10^{-4}$ K^{-1}. Although these absolute values are very approximate, the *signs* of both parameters indicate that the spectral weight is taken from the region above 2.5 eV and added to the region below 0.8 eV.

III. SLOPE-DIFFERENCE SPECTRAL ANALYSIS

Now we present the full data analysis without using the approximation (7). The technique we present here is a modification of the temperature-modulation spectroscopy.[33,34,46] Because of the KK relation (5), we can model the slope-difference dielectric function with the following dispersion formula:

$$\Delta_s\epsilon(\omega) = \Delta_s\epsilon_\infty + \sum_{i=0}^{N}\frac{A_i}{\omega_i^2-\omega^2-i\gamma_i\omega}. \qquad (8)$$

$\Delta_s\epsilon_\infty$ is responsible for the high-frequency electronic excitations, while each Lorentzian term represents either an addition or a removal of spectral weight, depending on the sign of A_i. We emphasize that this model is just a parametrization.

TABLE I. Model parameters of $\Delta_s\epsilon(\omega)$ by formula (8) which correspond to the best fit of the experimental data. $\Delta_s\epsilon_\infty=-3.1\times10^{-5}$ K^{-1}.

i	ω_i (cm^{-1})	A_i (10^5 cm^{-2} K^{-1})	γ_i (cm^{-1})
0	0	2.82	0
1	0	−11.25	3977
2	582	−2.40	488
3	939	2.20	707
4	2078	6.51	4496
5	2082	2.60	6141
6	3543	−0.17	1685

The number of oscillators, N, has to be chosen in order to get a good fit of experimental data. The physical meaning of some oscillators, taken alone, may not be well defined. However, the essential feature of the functional form (8) is that it preserves[47] the KK relation (5).

We include the infrared $\Delta_s R(\omega)$ to the fitting procedure by making use of the following relation:[11,46]

$$\Delta_s R(\omega) = \frac{\partial R}{\partial\epsilon_1}(\omega,T_c)\Delta_s\epsilon_1(\omega) + \frac{\partial R}{\partial\epsilon_2}(\omega,T_c)\Delta_s\epsilon_2(\omega)$$
$$= 2R(\omega,T_c)\mathrm{Re}\left[\frac{\Delta_s\epsilon(\omega)}{\sqrt{\epsilon(\omega,T_c)}[\epsilon(\omega,T_c)-1]}\right]. \qquad (9)$$

The method which we use to determine the "sensitivity functions" $(\partial R/\partial\epsilon_{1,2})(\omega,T_c)$ from the experimental data is described in Appendix B.

The green solid lines in Figs. 3(a) and 3(b) denote the best fit[48] of $\Delta_s\epsilon_1(\omega)$ and $\Delta_s\epsilon_2(\omega)$ and, *simultaneously*, $\Delta_s R(\omega)$. One can see that all essential spectral details are well reproduced. The corresponding parameter values are collected in Table I. The first oscillator in Eq. (8) combines the condensate and the narrow ($\gamma<100$ cm^{-1}) quasiparticle peak, while the remaining oscillators mimic the redistribution of spectral weight at finite frequencies.

The slope-difference integrated spectral weight for the model (8),

$$\Delta_s W(\omega) = \frac{A_0}{8} + \int_{0+}^{\omega}\Delta_s\sigma_1(x)dx, \qquad (10)$$

is presented as a solid green curve in Fig. 3(c). It gives $\Delta_s W(\Omega_c)\approx+770\ \Omega^{-1}\,\mathrm{cm}^{-2}\,\mathrm{K}^{-1}$, which is about 2 times larger than the rough estimate in Sec. IV.

In order to test how robust this result is, we did two more fits of the same data, with an extra imposed constraint that either (i) $\Delta_s W(\Omega_c)=0$ or (ii) $\Delta_s W(\Omega_c)=-770\ \Omega^{-1}\,\mathrm{cm}^{-2}\,\mathrm{K}^{-1}$. The resulting "best-fitting" curves are shown in Figs. 3(a)–3(c) as dashed blue and dotted red, respectively. One can clearly see that the models with $\Delta_s W(\Omega_c)\leqslant 0$ fail to reproduce the experimental spectra, most spectacularly the high-frequency spectrum of $\Delta_s\epsilon_1(\omega)$. This is not surprising, since the imposed constraint changes the sign of the leading term $\sim\omega^{-2}$ in formula (7).

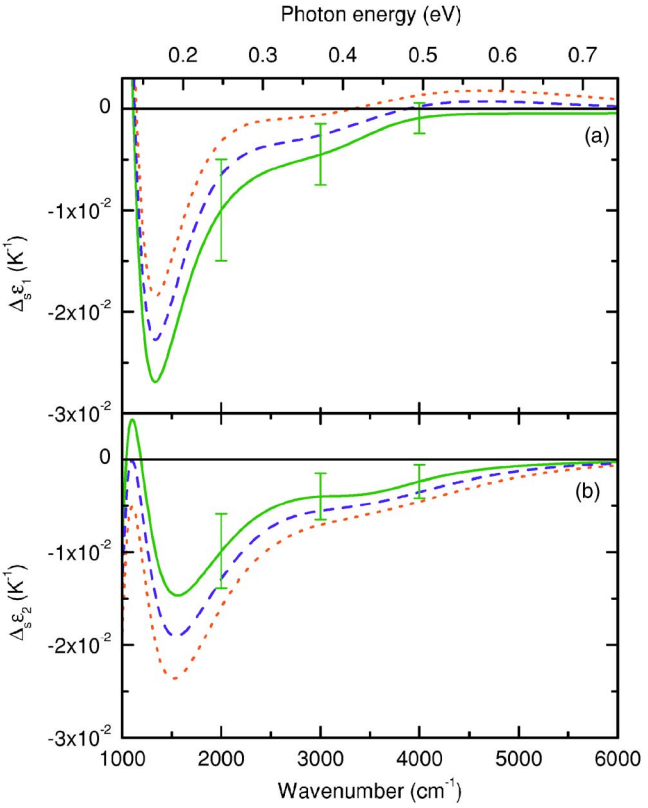

FIG. 4. (Color online) The continuation of the model slope-difference curves $\Delta_s\epsilon_1(\omega)$ (a) and $\Delta_s\epsilon_2(\omega)$ (b) of Fig. 3(b) to the midinfrared region, where only the reflectivity was measured. The colors and types of curves correspond to the ones in Fig. 3 (namely, the solid green curve is the best fit of all data, without any assumptions about the integrated spectral weight, while the dashed blue and dotted red curves are the fits with artificial constraints on the spectral weight). Note that the error bars, which are estimated as described in the text, are significantly increasing as the frequency is lowered.

To exclude the possibility that the failure to get a good fit with the mentioned constraint would be a spurious result caused by the limited number of Lorentz oscillators used for fitting the data, we have also used the KK-constrained variational dielectric model,[35] which is, in simple terms, a collection of a large number of adjustable oscillators, uniformly distributed in the whole spectral range, including the region above 2.5 eV. Thus we are confident that the dispersion model is able to reproduce all significant spectral features of the true function $\Delta_s\epsilon_1(\omega)$. However, these efforts did not improve the quality of the fit.

From this analysis we conclude that our experimental data *unequivocally* reveal the superconductivity-induced increase of $W(\Omega_c,T)$ in optimally doped Bi2212, confirming the statements given in Refs. 1 and 2.

In Fig. 4 the model curves of $\Delta_s\epsilon_1(\omega)$ and $\Delta_s\epsilon_2(\omega)$ from Fig. 3(b) are extended into the midinfrared range, where only the reflectivity was measured. The indicated error bars were estimated using the following criterium: when $\Delta_s\epsilon_{1,2}(\omega)$ is varied within these limits, a satisfactory fit of the measured $\Delta_sR(\omega)$ and $\Delta_s\epsilon_{1,2}(\omega)$ can still be achieved. Quite naturally, the uncertainty increases as the frequency is lowered. One can see that the trend of negative $\Delta_s\epsilon_1(\omega)$ is continued down to 0.2 eV, with a possible exception in the region near 0.5 eV, where error bars do not allow one to conclude about the sign of $\Delta_s\epsilon_1(\omega)$. In Ref. 3, the temperature dependence of the frequency-averaged ϵ_1 between 0.25 and 0.4 eV of slightly underdoped Bi2212 was presented (Fig. S6). Although this plot does not exclude the possibility that $\langle\epsilon_1\rangle$ has a kink (slope change) at T_c in the range between -0.001 K^{-1} and -0.002 K^{-1}, we obtain a kink value for the same averaged quantity, which is approximately 4 times larger. At this moment it is not clear whether this discrepancy, which appears to be of a quantitative rather than of a qualitative nature, is related to a sample issue or to the differences in the experimental procedure.

An alternative approach is to fit the total set of spectra at every temperature[1,49] using a certain KK-consistent model with temperature-dependent parameters. There is a variety of possibilities to parametrize the dielectric function. However, it was shown by one of us[49] that every model which reproduces satisfactorily not only the spectral features, but also the temperature dependence of the directly measured $R(\omega)$ and $\epsilon(\omega)$, gives a net increase of the low-frequency spectral weight below T_c.

IV. DISCUSSION

A. Absolute change of the spectral weight

Having found that the integrated spectral weight $W(\Omega_c,T)$ exhibits an extra *increase* below T_c, we want to evaluate its *absolute* superconductivity-induced change, continued into the low-temperature region:

$$\Delta W(\Omega_c,T) \equiv W(\Omega_c,T) - W_n(\Omega_c,T), \tag{11}$$

where $W_n(\Omega_c,T)$ is the "correct" extrapolation of the normal-state curve below T_c. In principle, $W_n(\Omega_c,T)$ can be measured when the superconducting order parameter is suppressed by an extremely high magnetic field (of the order of hundreds of teslas). Unfortunately, such large fields are currently prohibitive for accurate optical experiments.

However, an order-of-magnitude estimate and, simultaneously, an upper limit of $\Delta W(\Omega_c,T)$ at zero temperature can be obtained by the formula

$$\Delta W(\Omega_c,0) \sim T_c\Delta_s W(\Omega_c). \tag{12}$$

This gives $\Delta W(\Omega_c,0K) \sim 7\times10^4\ \Omega^{-1}\,\mathrm{cm}^{-2}$, which is about 1% of the total low-frequency spectral weight $W(\Omega_c,0K) \approx 7\times10^6\ \Omega^{-1}\,\mathrm{cm}^{-2}$. Since the temperature dependence of $\Delta W(\Omega_c,T)$ is expected to saturate somewhat below T_c, a more realistic estimate is smaller by about a factor of 2–5—i.e., between 0.2% and 0.5% of $W(\Omega_c,0K)$. These rough margins are suggested by the temperature dependence of the *ab*-plane[50] and *c*-axis[8] penetration depths.

If we assume that $\Delta_s W(\Omega_c)$ reflects largely the change of the intraband spectral weight (see Sec. IV B), then, according to Eq. (2), the corresponding lowering of the kinetic energy E_{kin} is 0.4–1 meV per Cu atom.[1] This amount is large

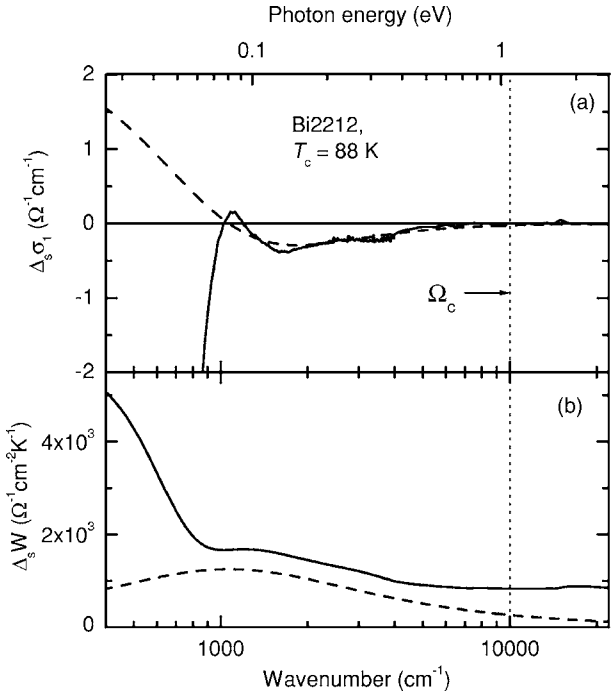

FIG. 5. (a) Slope-difference conductivity $\Delta_s\sigma_1(\omega)$ of optimally doped Bi2212. (b) The corresponding integrated spectral weight $\Delta_s W(\omega)$. The dashed lines show a model which mimics the narrowing of the Drude peak.

enough to account for the condensation energy of about 0.25 meV (Ref. 42) in optimally doped Bi2212. However, we should remember that Eq. (2) is strictly valid only in the context of the nearest-neighbor tight-binding model [see also the footnote (32) in Ref. 1].

B. Origin of the spectral weight transfer

A legitimate question is whether the observed increase of $W(\Omega_c,T)$ below T_c is due to the transfer of SW from the interband transitions to the intraband (Drude) conductivity—i.e., by the increase of $W_{intra}(T)$—or is simply caused by an extra narrowing of the Drude peak in the SC state,[3,39] without changing $W_{intra}(T)$. The distinction between the intraband and interband spectral weights can be made in theoretical models, but in experimental spectra their separation is not unique, because of the unavoidable overlap between these spectral ranges. Nevertheless, the temperature and spectral behavior of the optical constants suggests a likely scenario.

Figure 5(a) shows the slope-difference conductivity $\Delta_s\sigma_1(\omega)$, which is obtained by the most detailed multioscillator fit[35] of the data, shown in Fig. 3. The decrease of $\sigma_1(\omega)$ below T_c in the frequency range from 0.15 to about 0.8 eV is due to an extra narrowing of the Drude peak, caused by the reduced charge carrier scattering in the superconducting state. In the most crude model where the intraband peak is described by the Drude formula $\sigma_1(\omega)=(4\pi)^{-1}\omega_p^2\gamma(\omega^2+\gamma^2)^{-1}$ and the superconductivity-induced narrowing is given by a simple change of γ, we get $\Delta_s\sigma_1(\omega)=(4\pi)^{-1}\omega_p^2(\omega^2-\gamma^2)(\omega^2+\gamma^2)^{-2}\Delta_s\gamma$. This shape (with $\gamma=0.14$ eV) matches the experimental curve above 0.15 eV quite well, even though the real shape of the conductivity peak is much more complicated. Below 0.12 eV the drop of the conductivity is caused by the opening of the SC gap. Thus, a peak of $\Delta_s\sigma_1(\omega)$ at 0.13–0.14 eV, where the SC-induced change of σ_1 is even positive, is probably a cooperative effect of the narrowing of the Drude peak and the suppression of conductivity in the gap region. This peak corresponds to a dip in the spectrum $\Delta_s R(\omega)$ [Fig. 3(a)].

Figure 5(b) depicts $\Delta_s W(\omega)$, which is obtained by the integration of $\Delta_s\sigma_1(\omega)$ of Fig. 5(a). There is almost no superconductivity-induced change of $\sigma_1(\omega)$ above 0.8 eV up to at least 2.5 eV. Correspondingly, $\Delta_s W(\omega)$ is a positive constant in this region [Fig. 3(c)], showing that the Ferrell-Glover-Tinkham sum rule (in the slope-difference representation) $\Delta_s W(\omega)=0$ is not satisfied even for ω well above 2.5 eV. Therefore, the scenario where the narrowing of the Drude peak is fully responsible for the observed SC-induced increase $\Delta_s W(\omega)$ requires an assumption that a large portion of the Drude peak extends to energies well above 2.5 eV. Given the fact that the bandwidth is about 2 eV, such a scattering rate seems to be unrealistically large. Accordingly, $\Delta_s W(\omega)$, which corresponds to the discussed Drude-narrowing model [dotted line in Fig. 5(b)] accounts for only about one-third of the actual value at the cutoff energy Ω_c. It suggests that, at least in optimally doped Bi2212, a more plausible explanation is a *superconductivity-induced spectral weight transfer from the interband transitions to the intraband peak*.

While the redistribution of SW below 2.5 eV is well determined in our measurements, the observation of the details of the interband spectral weight removal, which is most likely spread over a very broad range of energies, is beyond our experimental accuracy at the moment.

C. Comparison with other measurements

It is interesting to compare the spectral weight transfer for different doping levels and in different high-T_c compounds. The temperature-dependent optical spectra of underdoped Bi2212 (T_c=66 K) show similar trends,[1,49] as the ones of the optimally doped sample, pointing towards the superconductivity-induced increase of the low-frequency spectral weight, opposite to the BCS scenario. However, the kinks at T_c in the underdoped sample are not as sharp as in the optimally doped one, which might be caused by a broadening of the fluctuation region around T_c in the pseudogap regime.

A surprising result came recently from the overdoped region. The analysis of overdoped Bi2212 films (T_c=63 K) revealed a superconductivity-induced spectral weight reduction[13]—i.e., a change which is opposite to optimally doped and underdoped Bi2212—reported in Refs. 1 and 2. The authors concluded that if a single mechanism is responsible for superconductivity across the whole phase diagram, this mechanism should allow for a smooth transition between the two regimes around optimal doping.

Recently superconductivity-induced reduction of low frequency spectral weight was reported by Boris *et al.*[3] for op-

timally doped Y123 (T_c=92.7 K) and slightly underdoped Bi2212 (T_c=86 K). With respect to Bi2212, these conclusions contradict those of Refs. 1 and 2, unless one assumes that the sign change is due to a small difference in the doping levels. Given the fact the in both optimally doped (T_c =88 K) and in the underdoped (T_c=66 K) samples of Bi2212 the same effect was observed,[1] the latter possibility seems rather unlikely. However, the conclusions of Ref. 3 were based on the temperature independence of $\epsilon_1(\omega)$ below T_c above 0.25 eV (see Refs. 51 and 52 for a detailed discussion), whereas our analysis shows a distinct extra decrease of ϵ_1 below T_c, compared to the normal-state trends [see the negative value of $\Delta_s\epsilon_1$ in Figs. 3(b) and 4]. Since no temperature-dependent spectra on Bi2212 were presented above 0.5 eV, it currently remains unclear whether a similar slope-difference analysis of the data from Ref. 3 would actually lead to the opposite conclusion regarding the superconductivity-induced spectral weight transfer.[51]

Although the authors of Ref. 3 applied the same arguments to the case of Y123 as to Bi2212, we note here that the temperature-dependent curves of ϵ_1 on Y123 (but not on Bi2212) show an upward kink at T_c [i.e., opposite to our data of Bi2212—e.g., those shown in Figs. 2(a), 3(b), and 4(a)], which indeed suggests the decrease of the low-frequency spectral weight below T_c (see Figs. 1 C-F, S3 B, and S6 A of Ref. 3). Interestingly, the kink is much stronger in the *b* direction (parallel to the chains), showing the importance of the chains in the process of the spectral weight transfer.

Taken together, the results of various groups imply that the direction and the amount of the spectral weight transfer in cuprates are determined by different aspects of these materials, such as the level of the doping and the nature of the doping reservoirs (chains in the case of Y123 can play a role as well). This calls for further doping-dependent studies of various cuprate families combined with realistic calculations, beyond Eq. (2), of the spectral weight transfer within competing superconductivity scenarios taking into account the actual band parameters of individual materials.

V. SUMMARY

We presented a detailed analysis of the superconductivity-induced redistribution of spectral weight in optimally doped Bi2212 by applying a modified temperature-modulation technique[33] to the published earlier optical data.[1] By taking advantage of a high-temperature resolution, we determine the kinks (slope changes) at T_c of directly measured optical quantities—reflectivity $R(\omega)$ below 0.75 eV and ellipsometrically measured $\epsilon_1(\omega)$ and $\epsilon_2(\omega)$ at higher energies. The Kramers-Kronig constrained modeling of the slope-difference spectra clearly shows an extra gain of the low-frequency integrated SW as a result of the superconducting transition. Moreover, an artificially imposed condition of the opposite sign of the spectral weight change is incompatible with the experimental data, most importantly with the changes of the dielectric function between 0.8 and 2.5 eV. Qualitatively, one of the hallmarks of the SC-induced increase of the low-frequency spectral weight is an extra decrease below T_c of high-frequency ϵ_1, as compared to the normal-state trends.

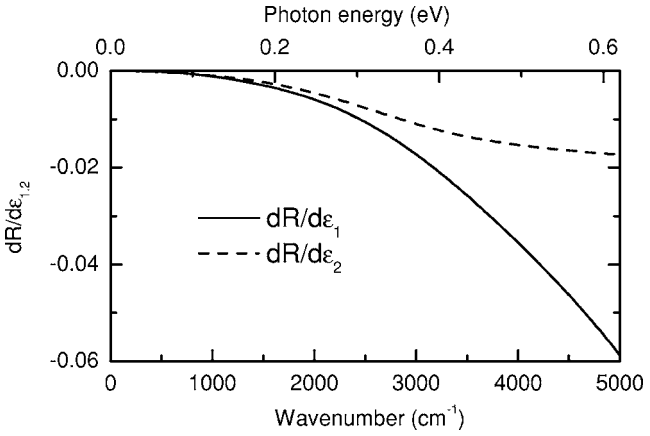

FIG. 6. The "sensitivity functions" $(\partial R/\partial\epsilon_1)(\omega)$ and $(\partial R/\partial\epsilon_2)\times(\omega)$ in the near and far infrared, obtained for Bi2212 near optimal doping at T_c=88 K as described in Appendix B.

The increased low-frequency SW is not compensated at 2.5 eV and somewhat higher energies; this suggests that this is mostly caused by the spectral weight transfer from the interband towards intraband transitions and only partially by the narrowing of the Drude peak. This implies that the electronic kinetic energy decreases in the superconducting state, which is opposite to the BCS scenario.

Further experiments should help in completing the general picture of the SC-induced spectral weight transfer in different parts of the phase diagram of the high-T_c cuprates.

ACKNOWLEDGMENTS

The authors wish to thank A. F. Santander-Syro, N. Bontemps, G. Deutscher, J. Orenstein, M. R. Norman, B. Keimer, C. Bernhard, and A. V. Boris for fruitful discussions. This work was supported by the Swiss National Science Foundation through the National Center of Competence in Research Materials with Novel Electronic Properties-MaNEP.

APPENDIX A: DETERMINATION OF $\Delta_s R(\omega)$ AND $\Delta_s\epsilon_{1,2}(\omega)$

According to the definition (4), the determination of $\Delta_s R(\omega)$ involves the calculation of $\partial R(T)/\partial T$ above and below T_c. The numerical derivatives, calculated straightforwardly from the data points shown in Fig. 1, are rather noisy, with the exception of some frequencies, where the signal is especially good. In order to limit the statistical noise, we can take advantage of the large number of temperatures measured and use the following procedure. For each frequency, a curve $R(T)$ is fitted to a second-order polynomial $P_{low}(T)$ between T_{low} and T_c and another polynomial $P_{high}(T)$ between T_c and T_{high}, where $T_{low}<T_c$ and $T_{high}>T_c$ are some selected temperatures. For the optimally doped Bi2212 we used T_{low}=30 K, T_c=88 K, and T_{high}=170 K. The polynomial curves below and above T_c are shown by respectively

blue and red curves in Fig. 1. The superconductivity-induced slope change is calculated as

$$\Delta_s R = \left.\frac{dP_{high}(T)}{dT}\right|_{T_c} - \left.\frac{dP_{low}(T)}{dT}\right|_{T_c}. \quad \text{(A1)}$$

We estimate the error bars of $\Delta_s R$ by varying T_{low} and T_{high} in certain reasonable limits (20–40 K and 150–200 K, respectively). These error bars reflect mostly the systematic uncertainties of the numerical procedure. Exactly the same method was applied to determine $\Delta_s \epsilon_1(\omega)$ and $\Delta_s \epsilon_2(\omega)$ from the temperature-dependent curves shown in Fig. 2.

APPENDIX B: DETERMINATION OF $(\partial R/\partial \epsilon_{1,2})(\omega, T_c)$

The application of the slope-difference analysis in the range where only $R(\omega)$ is measured requires the knowledge of "sensitivity functions" $(\partial R/\partial \epsilon_{1,2})(\omega)$, taken at T_c. We determine them from a Drude-Lorentz model, which fits well both $R(\omega)$ and the ellipsometrically measured $\epsilon_1(\omega)$ and $\epsilon_2(\omega)$ at higher frequencies. The accuracy in this case is superior to the usual KK transform of reflectivity, since the high-frequency ellipsometry data effectively "anchor" the phase of R at low frequencies.[35,44] The result is shown in Fig. 6. Both $(\partial R/\partial \epsilon_1)(\omega, T_c)$ and $(\partial R/\partial \epsilon_1)(\omega, T_c)$ are rather structureless and vanishing, as ω goes to 0.

[1] H. J. A. Molegraaf, C. Presura, D. van der Marel, P. H. Kes, and M. Li, Science **295**, 2239 (2002).
[2] A. F. Santander-Syro, R. P. S. M. Lobo, N. Bontemps, Z. Konstatinovic, Z. Z. Li, and H. Raffy, Europhys. Lett. **62**, 568 (2003).
[3] A. V. Boris, N. N. Kovaleva, O. V. Dolgov, T. Holden, C. T. Lin, B. Keimer, and C. Bernhard, Science **304**, 708 (2004).
[4] J. Schützmann, H. S. Somal, A. A. Tsvetkov, D. van der Marel, G. E. J. Koops, N. Koleshnikov, Z. F. Ren, J. H. Wang, E. Brück, and A. A. Menovsky, Phys. Rev. B **55**, 11118 (1997).
[5] K. A. Moler, J. R. Kirtley, D. G. Hinks, T. W. Li, and Ming Xu, Science **279**, 1193 (1998).
[6] A. A. Tsvetkov, D. van der Marel, K. A. Moler, J. R. Kirtley, J. L. de Boer, A. Meetsma, Z. F. Ren, N. Koleshnikov, D. Dulic, A. Damascelli, M. Grüninger, J. Schützmann, J. W. van der Eb, H. S. Somal, and J. H. Wang, Nature (London) **395**, 360 (1998).
[7] J. R. Kirtley, K. A. Moler, G. Villard, and A. Maignan, Phys. Rev. Lett. **81**, 2140 (1998).
[8] M. B. Gaifullin, Yuji Matsuda, N. Chikumoto, J. Shimoyama, K. Kishio, and R. Yoshizaki, Phys. Rev. Lett. **83**, 3928 (1999).
[9] D. N. Basov, S. I. Woods, A. S. Katz, E. J. Singley, R. C. Dynes, M. Xu, D. G. Hinks, C. C. Homes, and M. Strongin, Science **283**, 49 (1999).
[10] A. V. Boris, D. Munzar, N. N. Kovaleva, B. Liang, C. T. Lin, A. Dubroka, A. V. Pimenov, T. Holden, B. Keimer, Y.-L. Mathis, and C. Bernhard, Phys. Rev. Lett. **89**, 277001 (2002).
[11] A. B. Kuzmenko, N. Tombros, H. J. A. Molegraaf, M. Grüninger, D. van der Marel, and S. Uchida, Phys. Rev. Lett. **91**, 037004 (2003).
[12] D. van der Marel, in *Strong Interactions in Low Dimensions*, edited by D. Baeriswyl and L. Degiorgi(Kluwer, Dordrecht, 2005); cond-mat/0301506
[13] G. Deutscher, A. F. Santander-Syro, and N. Bontemps, cond-mat/0503073 (unpublished).
[14] J. E. Hirsch, Physica C **201**, 347 (1992).
[15] P. W. Anderson, Science **268**, 1154 (1995).
[16] A. J. Leggett, Science **274**, 587 (1996).
[17] S. Chakravarty, Eur. Phys. J. B **5**, 337 (1998).
[18] S. Chakravarty, Hae-Young Kee, and E. Abrahams, Phys. Rev. Lett. **82**, 2366 (1999).
[19] D. Munzar, C. Bernhard, T. Holden, A. Golnik, J. Humlicek, and M. Cardona, Phys. Rev. B **64**, 024523 (2001).
[20] D. Munzar, T. Holden, and C. Bernhard, Phys. Rev. B **67**, 020501(R) (2003).
[21] M. R. Norman and C. Pépin, Phys. Rev. B **66**, 100506(R) (2002).
[22] D. van der Marel, H. J. A. Molegraaf, C. Presura, and I. Santoso, in *Concepts in Electron Correlation*, edited by A. Hewson and V. Zlatic (Kluwer, Dordrecht, 2003).
[23] A. Knigavko, J. P. Carbotte, and F. Marsiglio, Phys. Rev. B **70**, 224501 (2004).
[24] A. Abanov and A. V. Chubukov, Phys. Rev. B **70**, 100504(R) (2004).
[25] L. Benfatto, S. G. Sharapov, and H. Beck, Eur. Phys. J. B **39**, 469 (2004).
[26] P. W. Anderson, P. A. Lee, M. Randeria, T. M. Rice, N. Trivedi, and F. C. Zhang, J. Phys.: Condens. Matter **16**, R755 (2004).
[27] J. E. Hirsch, Phys. Rev. B **69**, 214515 (2004).
[28] T. D. Stanescu and P. Phillips, Phys. Rev. B **69**, 245104 (2004).
[29] T. A. Maier, M. Jarrell, A. Macridin, and C. Slezak, Phys. Rev. Lett. **92**, 027005 (2004).
[30] B. Farid, Philos. Mag. **84**, 109 (2004).
[31] P. Wrobel, R. Eder, and P. Fulde, J. Phys.: Condens. Matter **15**, 6599 (2003).
[32] P. F. Maldague, Phys. Rev. B **16**, 2437 (1977).
[33] M. Cardona, *Modulation Spectroscopy* (Academic, New York, 1969).
[34] M. J. Holcomb, J. P. Collman, and W. A. Little, Phys. Rev. Lett. **73**, 2360 (1994).
[35] A. B. Kuzmenko, Rev. Sci. Instrum. **76**, 083108 (2005).
[36] M. Ortolani, P. Calvani, and S. Lupi, Phys. Rev. Lett. **94**, 067002 (2005).
[37] A. Toschi, M. Capone, M. Ortolani, P. Calvani, S. Lupi, and C. Castellani, cond-mat/0502528 (unpublished).
[38] D. van der Marel, H. J. A. Molegraaf, J. Zaanen, Z. Nussinov, F. Carbone, A. Damascelli, H. Eisaki, M. Greven, P. H. Kes, and M. Li, Nature (London) **425**, 271 (2003).
[39] A. E. Karakozov, E. G. Maksimov, and O. V. Dolgov, Solid State Commun. **124**, 119 (2002).
[40] M. Rübhausen, A. Gozar, M. V. Klein, P. Guptasarma, and D. G. Hinks, Phys. Rev. B **63**, 224514 (2001).
[41] A. Junod, A. Erb, and C. Renner, Physica C **317**, 333 (1999).
[42] J. W. Loram, J. Luo, J. R. Cooper, W. Y. Liang, and J. L. Tallon, J. Phys. Chem. Solids **62**, 59 (2001).
[43] In Bi2212, one observes that the temperature-dependent quantities such as the entropy $S(T)$ do not have a real kink, but rather

an inflection point at T_c. Correspondingly the specific heat dS/dT has a λ-like maximum at T_c instead of a sharp specific heat jump. Fitting the temperature dependence over some finite temperature range above and below T_c with a second-order polynomial and taking the slope difference, as we do, measures the slope change over the fluctuation region around T_c. If the fluctuation region becomes too broad, it becomes increasingly difficult to separate the superconductivity-induced effects from the normal-state trends. For Bi2212 near optimal doping, considered here, the fluctuation region is sufficiently narrow (see Ref. 53), allowing an unproblematic and meaningful kink analysis.

[44] I. Bozovic, Phys. Rev. B **42**, 1969 (1990).

[45] Although the formulas of this paper are given in the Gaussian system of units, the values of σ_1 and W are presented in the practical units (Ω^{-1} cm^{-1} and Ω^{-1} cm^{-2}, respectively).

[46] O. V. Dolgov, A. E. Karakozov, A. M. Mikhailovsky, B. J. Feenstra, and D. van der Marel, Physica C **229**, 6360 (1994).

[47] The only requirement for the KK consistency of the dispersion model (8) is that all $\gamma_i \geqslant 0$.

[48] All data modeling was done using an automated nonlinear fitting routine, implemented in REFFIT software (http://optics.unige.ch/alexey/reffit.html).

[49] H. J. A. Molegraaf, Ph.D. thesis, Rijksuniversiteit Groningen, 2005. Available on-line at http://irs.ub.rug.nl/ppn/271449179

[50] Shih-Fu Lee, D. C. Morgan, R. J. Ormeno, D. M. Broun, R. A. Doyle, J. R. Waldram, and K. Kadowski, Phys. Rev. Lett. **77**, 735 (1996).

[51] A. B. Kuzmenko, H. J. A. Molegraaf, F. Carbone, and D. van der Marel, cond-mat/0503768 (unpublished).

[52] A. F. Santander-Syro and N. Bontemps, cond-mat/0503767 (unpublished).

[53] J. Corson, R. Mallozzi, J. Orenstein, J. N. Eckstein, and I. Bozovic, Nature (London) **398**, 221 (1999).